

GLOBAL KINETICS FOR *n*-HEPTANE IGNITION AT HIGH PRESSURES

U. C. MÜLLER AND N. PETERS

*Institut für Technische Mechanik
Rheinisch-Westfälische Technische Hochschule Aachen
Federal Republic of Germany*

AND

A. LIÑÁN

*Dpto. Motopropulsion y Thermofluidodinamica
Universidad Politécnica de Madrid, Spain*

A kinetic mechanism of 1011 elementary reactions with 171 chemical species for *n*-heptane ignition is analysed and reduced to 4 global steps with adjusted rate coefficients to describe ignition at pressures around 40 atm. Two of these steps account for the high temperature branch and the other two for the low temperature branch of the ignition mechanism. The ignition delay time passes through a negative temperature dependence during the transition between the two branches. This is accounted for by the reversible third reaction step, which models the first and second O₂-addition in the degenerated chain branching mechanism at low temperatures. Ignition delay times calculated with the adjusted 4-step model are compared to those from the detailed kinetics and experimental data. Finally the 4-step mechanism is analysed by asymptotic methods and explicit ignition delay time formulas are derived.

Introduction

Auto-ignition plays a central part in many practical combustion systems burning hydrocarbon fuels. One example is the ignition of the fuel spray in a Diesel engine, another is the auto-ignition of the end gas in a spark ignition engine. While a short ignition delay time is desirable in the Diesel engine, it is undesirable in the spark ignition engine since it may lead to the onset of engine knock and therefore to knock damage.

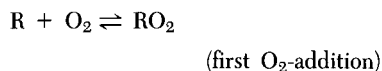
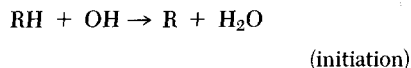
Ignition of higher hydrocarbon fuel typically exhibits two distinctly different regimes:^{1,2,3}

1. the high temperature regime where the fuel is rapidly decomposed into small C₂- and C₁-hydrocarbons, which are subsequently oxidized;
2. the low temperature regime where the fuel is oxidized by O₂-addition in a degenerated chain branching.

Rather detailed mechanisms have been proposed to model the ignition delay times of fuels like *n*-heptane and iso-octane over a large temperature range.^{1,4,5,6} Some reduced ad-hoc models also have been proposed to describe the basic chemical interactions in a conceptually more accessible form.^{4,7,8,9} Only recently, however, reliable experimental data for *n*-heptane ignition have been produced by experiments in a large shock tube with sufficiently large residence times of an undisturbed

mixture behind the reflected shock.¹⁰ These data were used to adjust the elementary kinetic parameters, in particular those of the low temperature chemistry.^{3,11} This led to a reaction mechanism of 1011 elementary reactions with 171 chemical species for the *n*-heptane ignition chemistry. Figure 1 shows that the full kinetics reproduce the ignition delay times of the experimental data¹⁰ quite well. This mechanism was analysed with respect to the sensitivity of ignition delay times of the individual reactions.

The high temperature oxidation proceeds from the attack on the fuel by H, OH and HO₂ radicals to form *n*-heptyl radicals and through the break-up of these into C₂H₄, CH₃ and H radicals. These are oxidized by reactions of the well-known C₁-C₂-chemistry. An essential feature of low temperature ignition of aliphatic hydrocarbons is the existence of a negative temperature dependence of ignition delay times in the intermediate temperature range as seen in Fig. 1. The chemistry for temperatures lower than 1000 K is characterized by degenerated chain branching which may be illustrated by the following sequence of reaction steps:



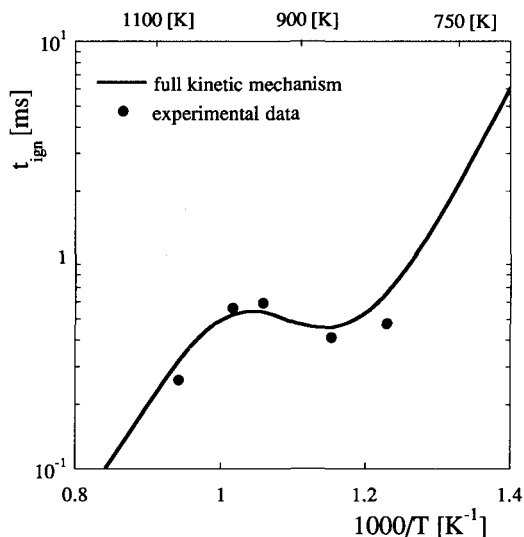
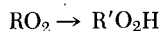
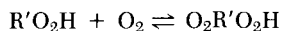


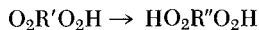
FIG. 1. Comparison of calculated ignition delay times of the full kinetics with experimental data¹⁰ at 40 atm and a stoichiometric *n*-heptane/air mixture.



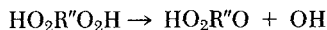
(internal H-abstraction)



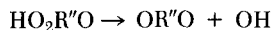
(second O₂-addition)



(internal H-abstraction)



(chain propagation)



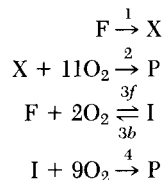
(chain branching)

For *n*-heptane R is represented by C₇H₁₅, R' = C₇H₁₄ and R'' = C₇H₁₃. The competition of the reverse reaction of the first O₂-addition with the subsequent internal H-abstraction is the key to understanding the negative temperature dependence of ignition delay.

The Adjusted Four-Step Mechanism

Since a large number of the intermediate species remains at low concentrations, it is possible to introduce steady state assumptions for these intermediates and thus to derive a systematically reduced mechanism.¹² Such a mechanism results in approximately 16 global reactions, which are controlled by the original elementary kinetic rate data.¹³

Here, however, we want to retain only the essential information from the chemistry and present a 4-step model with adjusted rate coefficients, which is written as



Here F stands for the fuel, with F = *n*-C₇H₁₆. X and I represent the combined intermediates, where X = 3C₂H₄ + CH₃ + H and I = HO₂R''O + H₂O. P represents a combination of the products, with P = 7CO₂ + 8H₂O.

The first two reactions correspond to a two-step high temperature scheme containing an endothermic fuel decomposition into small hydrocarbons and the exothermic oxidation of these into the final combustion products. The last two steps represent the degenerated chain branching mechanism discussed above. Steady state assumptions for all intermediates in this chain mechanism up to HO₂R''O lead to the third global step of the model. The fourth step contains the chain branching and the oxidation to the combustion products. Only the third reaction is considered to be reversible. The activation energy of the backward reaction 3*b* is assumed much larger than that of the forward reaction 3*f*. Therefore, at low temperatures the backward reaction 3*b* is unimportant. However, at temperatures around 830 K and higher, the backward reaction dominates over the forward reaction and thereby decreases the relative importance of reactions 3 and 4 in the mechanism. This explains the transition from the low temperature to the high temperature branch. The rate coefficients and the thermodynamic data to be used are given below.

In writing the conservation equations for this mechanism we shall assume, for the simplicity of the presentation, that the mean molecular mass and the specific heat at constant pressure are constant. Thus the conservation equations for the mole fractions X_F, X_X, X_I and X_O of F, X, I and O₂ take the form:

$$\frac{d}{dt} X_F = -k_1 X_F - k_{3f} X_F X_O + k_{3b} X_I \quad (1)$$

$$\frac{d}{dt} X_X = k_1 X_F - k_2 X_X X_O \quad (2)$$

$$\frac{d}{dt} X_I = k_{3f} X_F X_O - k_{3b} X_I - k_4 X_I X_O \quad (3)$$

$$\frac{d}{dt} (X_O - 11X_F - 11X_X - 9X_I) = 0 \quad (4)$$

The energy conservation equation can be written in the form

$$\frac{d}{dt} T = T_1 k_1 X_F + T_2 k_2 X_X X_O + T_3 (k_{3f} X_F X_O - k_{3b} X_I) + T_4 k_4 X_I X_O \quad (5)$$

Here the temperatures T_1 , T_2 , T_3 and T_4 take the values 20400 K, 149800 K, 1550 K and 127850 K. They were obtained by dividing the reacting enthalpies of the four different reactions by the constant pressure specific heat of the mixture, which was assumed to have a constant value of 34.8 (J/mol K). Notice that $T_1 + T_2 = T_3 + T_4$. Equations (1)–(3) and (5) can be combined to yield the conservation equation

$$\frac{d}{dt} \{T + (T_1 + T_2) X_F + T_2 X_X + (T_3 + T_4) X_I + T_4 X_O\} = 0 \quad (6)$$

The reaction constants appearing in Eqs. (1)–(3), have dimensions s^{-1} , and are given by

$$k_1 = A_1 e^{-E_1/RT}, \quad = \frac{p}{RT} A_2 e^{-E_2/RT},$$

$$k_{3f} = \frac{p}{RT} A_{3f} e^{-E_{3f}/RT} \quad k_{3b} = A_{3b} e^{-E_{3b}/RT},$$

$$k_4 = \frac{p}{RT} A_4 e^{-E_4/RT}$$

The factor p/RT in some of the reaction constants represents the number of moles per unit volume. The values for the activation temperatures E/R , and for the pre-exponential factors A , are

$$E_1/R = 21650 \text{ K}, \quad E_{3f}/R = E_1, \quad E_2 = E_1/3$$

$$E_{3b}/R = 37285 \text{ K}, \quad E_4/R = 13230 \text{ K}$$

and

$$A_1 = 1 \cdot 10^{10} (s^{-1}),$$

$$A_{3b} = 4 \cdot 10^{22} (s^{-1})$$

$$A_2 = 2 \cdot 10^{12} (cm^3 mol^{-1} s^{-1}),$$

$$A_{3f} = 3 \cdot 10^{18} (cm^3 mol^{-1} s^{-1}),$$

$$A_4 = 5 \cdot 10^{13} (cm^3 mol^{-1} s^{-1})$$

Equations (1)–(4) and (6) were integrated numerically using the initial conditions

$$t = 0; \quad X_F = X_{F,0} \quad X_O = X_{O,0}$$

$$X_X = X_I = 0, \quad T = T_0$$

The resulting ignition delay times are compared to those of a calculation using the full kinetics in Fig. 2. All calculations were made for a pressure of 40 atm and a stoichiometric fuel/air mixture. In general the 4-step mechanism agrees well with the full kinetic mechanism. The maximum error is less than 20% in the region of about 850 K. At different equivalence ratios ignition time depends more on the mole fraction of the fuel $X_{F,0}$ than on the mole fraction of the oxygen. In Fig. 3 the results of cal-

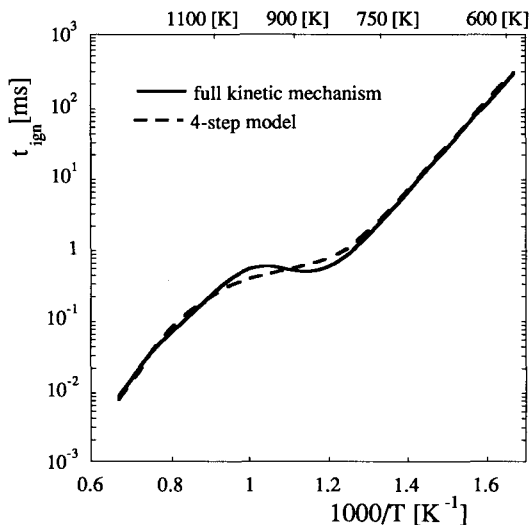


FIG. 2. Comparison of calculated ignition delay times of the full kinetics and those from the 4-step model at 40 atm and a stoichiometric *n*-heptane/air mixture.

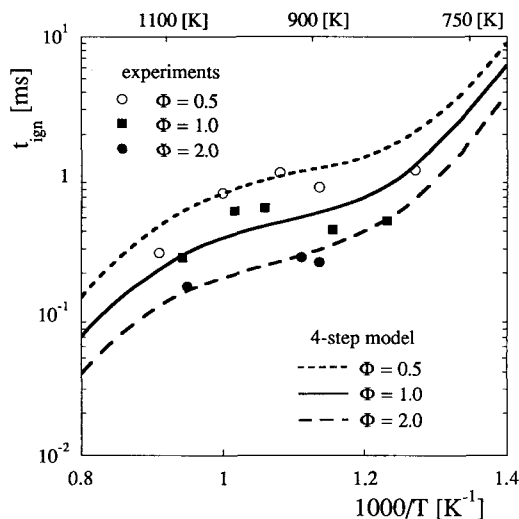
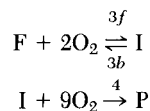


FIG. 3. Comparison of calculated ignition delay times of the 4-step model with experiments¹⁰ at 40 atm and different fuel/air equivalence ratios.

culations for different equivalence ratios are compared to experiments. Ignition delay times are larger for lean mixtures and lower for rich mixtures. The 4-step model also agrees well with the experimental data.¹⁰

Negative Temperature Dependence Branch:

Let us, for the moment, neglect the effects of reactions 1 and 2; we are left with the low temperature scheme



The conservation equations in this case simplify to

$$\frac{d}{dt} X_F = -k_{3f} X_F X_O + k_{3b} X_I \quad (7)$$

$$\frac{d}{dt} X_I = k_{3f} X_F X_O - k_{3b} X_I - k_4 X_I X_O \quad (8)$$

$$X_O - 11X_F - 9X_I = X_{O,0} - 11X_{F,0} \quad (9)$$

$$T + (T_3 + T_4)X_F + T_4 X_I = T_0 + (T_3 + T_4)X_{F,0} \quad (10)$$

Asymptotic Analysis of the Ignition Process

In order to understand the interaction between the different reactions of the 4-step mechanism, it is useful to compare the magnitude of the reaction rates in an Arrhenius diagram. Estimates of the reaction rates in Eqs. (1)–(3) can be obtained using values of X_F , X_O and T equal to their initial values $X_{F,0}$, $X_{O,0}$ and T_0 , and values for the mole fractions X_X and X_I of the intermediates equal to $X_{F,0}$.

The reaction rates, if we leave aside a factor $X_{F,0}$ to obtain a measure of the inverse of the reaction times of the five reactions, are

$$k_1, k_2 X_{O,0}, k_{3f} X_{O,0}, k_{3b}, \text{ and } k_4 X_{O,0}$$

where the reaction rates of the reactions 2, 3f and 4 include a factor p/RT , while the other rates are independent of the pressure.

Thus, if we consider as an example a stoichiometric mixture of *n*-heptane with air ($X_{F,0} = 0.0187$ and $X_{O,0} = 0.2061$) at a pressure of 40 atm, we obtain the reaction rates shown in Fig. 4 as functions of T_0 . Notice that these reaction rates are shifted upwards or downwards if the factor $pX_{O,0}$ appearing in the rates of the reactions 2, 3f, and 4 is changed.

The reaction times for the five reactions are seen to differ in order of magnitude; their ratios change with T_0 , changing from large to small or vice versa when T_0 passes through cross-over temperatures. The reaction rate of the first reaction is very small compared to the rate of the third reaction in the temperature range of interest in Diesel engine ignition. Thus the low temperature reaction path corresponding to reactions 3 and 4 appears to be favourable.

In Fig. 4 we see that for temperatures above 800 K the rate of reaction 4 is small compared to the rates of the two reactions 3. Under these conditions, there are two stages in the ignition process: In a first stage, with a characteristic time determined by the reactions 3, we can neglect the effect of reaction 4. No significant change of temperature occurs during this stage because T_3 is small compared to T_4 . The consumption of oxygen during this stage is also small because the partial stoichiometric coefficient 2 is small compared to 9. The temperature rise can only occur during the second stage,

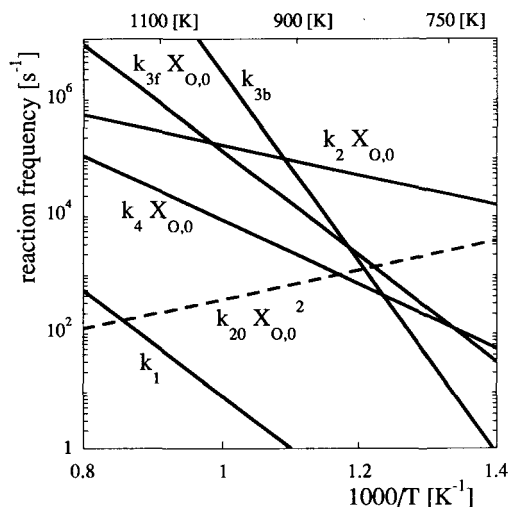


FIG. 4. Arrhenius diagram of the time scales of the different steps in the 4-step model.

when the fast reactions 3 are in partial equilibrium. In the long second stage, when the rise in temperature will take place, Eqs. (7) and (8) simplify to

$$k_{3f}X_OX_F = k_{3b}X_I \quad (11)$$

$$\frac{d}{dt}(X_I + X_F) = \frac{d}{dt}X_S = -k_4X_I X_O \quad (12)$$

If we define $X_S = X_I + X_F$, the mole fraction of the pool formed by I and F, then Eq. (11) leads to

$$X_I = X_S \frac{KX_O}{1 + KX_O} \quad (13)$$

where K is the equilibrium constant of the third reaction

$$K = \frac{k_{3f}}{k_{3b}} = \frac{p}{RT} \frac{A_{3f}}{A_{3b}} e^{(E_{3b} - E_{3f})/RT} \quad (14)$$

Thus Eq. (12) becomes

$$\frac{d}{dt}X_S = -k_4 \frac{KX_O}{1 + KX_O} X_O X_S \quad (15)$$

Since T_3 is small compared to $T_3 + T_4$ the temperature equation may be written as

$$\frac{dT}{dt} = (T_3 + T_4)k_4 \frac{KX_O}{1 + KX_O} X_O X_S \quad (16)$$

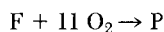
Equations (15) and (16) are to be solved with the relations (9) and (10) and the initial condition

$$t = 0: \quad X_S = X_{F,0}, \quad T = T_0$$

For values of T larger than the cross-over temperature of approximately 830 K, KX_O becomes small compared to 1. In this case the reverse reaction 3 is so fast that the concentration of I cannot grow: $X_I \ll 1$. Then $X_S = X_F$ and thus Eq. (15) simplifies to

$$\frac{d}{dt}X_F = -k_4K X_O^2 X_F \quad (17)$$

corresponding to the overall kinetic scheme



resulting from the steady state approximation for I. Note that the resulting expression for the overall rate is of second order with respect to X_O and of first order with respect to X_F . The reaction con-

stant

$$k_4 K = \left(\frac{p}{RT}\right)^2 \frac{A_{3f}}{A_{3b}} A_4 e^{-(E_4 + E_{3f} - E_{3b})/RT} \quad (18)$$

is associated with a negative activation temperature

$$(E_{3f} + E_4 - E_{3b})/R = -2370 \text{ [K]} \quad (19)$$

In summary, for temperatures significantly above 830 K, the overall rate of fuel consumption is given by

$$\frac{d}{dt}X_F = -\left(\frac{p}{RT}\right)^2 3.75 \cdot 10^9 e^{2370/T} X_O^2 X_F \quad (20)$$

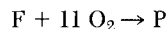
This rate is seen to decrease with increasing temperature, explaining the increase of the ignition time above 900 K. The reaction frequency

$$k_{20}X_{O,0}^2 = 3.75 \cdot 10^9 e^{2370/T} \left(\frac{p}{RT}\right)^2 X_{O,0}^2 \quad (21)$$

which is a measure of the inverse of the reaction time, is also plotted in Fig. 4 with a dashed line.

High Temperature Branch:

For temperatures larger than 1180 K the rate of fuel consumption by reactions 3 and 4, determined by (20), becomes smaller than the rate associated with reaction 1. Notice that at these high temperatures reaction 2 is very fast compared to reaction 1 and thus X follows the steady state approximation, being consumed as fast as it is produced. Reactions 1 and 2 can be replaced by the overall reaction



with the rate

$$\frac{d}{dt}X_F = -k_1X_F \quad (22)$$

Combining the effects of the two reaction paths the rate of fuel consumption for the entire temperature range (temperatures between 1500 K and 850 K) can with Eq. (17) and (22) be written as

$$\frac{d}{dt}X_F = -k_1X_F - k_4K X_F X_O^2 \quad (23)$$

Notice that the reaction rate dependence given by (23) leads to a minimum around 1180 K. With $T_1 + T_2 = T_3 + T_4$ the corresponding temperature equation is

$$\frac{dT}{dt} = (T_1 + T_2)(k_1 X_F + k_4 K X_F X_O^2) \quad (24)$$

Low Temperature Branch:

For temperatures lower than 800 K, reaction 3 is no longer in partial equilibrium and X_I is not determined by Eq. (11). However, the last term in Eq. (8) is small compared to either the first term (for low temperatures) or the second term (for temperatures around 850 K) and may therefore be neglected. Again there is a two-stage ignition process, where the fuel is partly converted to the intermediate I in the first stage. As in the negative temperature dependence branch, no significant heat release occurs during this stage. The subsequent consumption of I during the second stage is governed by the exothermic reaction 4 and leads to thermal runaway. Combining Eqs. (7) and (8) leads to the solution

$$X_F + X_I = X_{F,0} \quad (25)$$

Then Eq. (7) becomes

$$\frac{d}{dt} X_F = -(k_{3f} X_O + k_{3b}) X_F + k_{3b} X_{F,0} \quad (26)$$

which may be integrated to yield

$$X_F = X_{F,0} \left[e^{-kt} + \frac{1}{1 + KX_{O,0}} (1 - e^{-kt}) \right] \quad (27)$$

where $k = k_{3f} X_{O,0} + k_{3b}$, assuming constant temperature and $X_O = X_{O,0}$. Since $T_4 \gg T_3$ we cannot, however, neglect the heat release due to reaction 4. The temperature equation becomes in this limit

$$\frac{dT}{dt} = T_4 k_4 X_O (X_{F,0} - X_F) \quad (28)$$

Ignition, therefore, is due to the consumption of small amounts of X_I governed by reaction 4.

Calculation of Ignition Delay Times

At first only the temperature range between 1500 and 850 K is of interest. Due to the large exothermicity of the reactions, small changes in the fuel and oxygen concentration are sufficient to increase the temperature significantly. Accounting for the fact that the activation energy E_1 is large and that $(E_{3f} - E_{3b} + E_4)/RT_0$ is of order unity an expansion of

the temperature is given as

$$T = T_0 + \frac{RT_0^2}{E_1} \varphi \quad (29)$$

and neglecting the reactant consumption in Eq. (24) by setting $X_F = X_{F,0}$ and $X_O = X_{O,0}$ one obtains

$$\frac{d}{dt} \varphi = \frac{1}{t_1} e^\varphi + \frac{1}{t_2} \quad (30)$$

with the initial condition $\varphi(0) = 0$. At the ignition time φ becomes infinite

$$t_{ign} = t_2 \ln(1 + t_1/t_2) \quad (31)$$

Here

$$\frac{1}{t_1} = \left(\frac{E_1}{RT_0} \frac{T_1 + T_2}{T_0} X_{F,0} \right) A_1 e^{-E_1/RT_0} \quad (32)$$

$$\frac{1}{t_2} = \left(\frac{E_1}{RT_0} \frac{T_1 + T_2}{T_0} X_{F,0} \right) A_4 \frac{A_{3f}}{A_{3b}} \cdot e^{-(E_{3f} - E_{3b} + E_4)/RT_0} \left(\frac{p}{RT_0} X_{O,0} \right)^2 \quad (33)$$

For initial temperatures T_0 such that $KX_{O,0} \ll 1$ the ignition time is calculated according Eq. (31) together with the relations (32) and (33).

For temperatures significantly below 850 K the ignition time has to be calculated with the relations (27) and (28). Introducing the time variable

$$\begin{aligned} \tau &= \frac{KX_{O,0}}{1 + KX_{O,0}} \int_0^t (1 - e^{-kt}) dt \\ &= \frac{KX_{O,0}}{1 + KX_{O,0}} \left[t - \frac{1}{k} (1 - e^{-kt}) \right] \end{aligned} \quad (34)$$

Eq. (28) may be written as

$$\frac{dT}{d\tau} = T_4 k_4 X_O X_{F,0} \quad (35)$$

Thermal ignition occurs at

$$\frac{1}{\tau_{ign}} = \frac{E_4}{RT_0} \frac{T_4}{T_0} X_{F,0} X_{O,0} A_4 e^{-E_4/RT_0} \frac{p}{RT_0} \quad (36)$$

Eq. (34) may be inverted and approximated by a composite form satisfying small and large times as

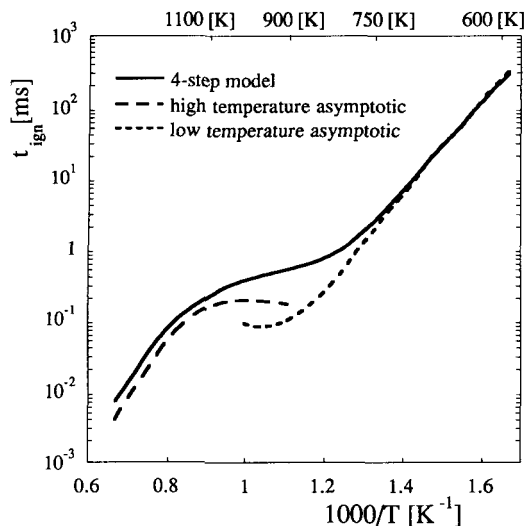


FIG. 5. Comparison of calculated ignition delay times of the 4-step model and asymptotic solutions at 40 atm and a stoichiometric *n*-heptane/air mixture.

$$t = \frac{1 + KX_{O,0}}{KX_{O,0}} \tau + \sqrt{\frac{2\tau}{k} \frac{1 + KX_{O,0}}{KX_{O,0}}} \quad (37)$$

Introducing $\tau = \tau_{ign}$ from Eq. (36) into Eq. (37) leads to the ignition time t_{ign} for the low temperature branch.

The resulting ignition times for the high temperature branch Eq. (31) and the low temperature branch Eq. (37) are compared to the numerical solution of the 4-step model in Fig. 5. The two asymptotic solutions describe qualitatively the general features of the full kinetic mechanism and both show the negative temperature dependence of ignition delay in the intermediate temperature range. The differences between the high temperature asymptotics and the 4-step numerical solution at temperatures above 1200 K are caused by the steady state assumption of the intermediate specie X and thereby by the neglect of the endothermic effects of the first reaction. At temperatures lower than 800 K the agreement of the low temperature asymptotics and the 4-step model is quite good. In the intermediate temperature range there is an interaction between the different regimes. The numerical solution does not separate the influence of the high and low temperature branch in the same way as the two asymptotic descriptions. This is the reason why the negative temperature dependence of the numerical 4-step solution in the intermediate range is missing.

Conclusion

A 4-step model with adjusted rate coefficients was derived that describes ignition at pressures around 40 atm. Ignition delay times calculated with the 4-step model and the full kinetics are in agreement with experiments. The maximum error in ignition delay between the two kinetic formulations is less than 20%. The dependence of ignition delay times on the equivalence ratio, calculated with the 4-step model, is satisfactory and also in agreement with experiments.

The mathematical structure of the 4-step mechanism has been studied by asymptotic analysis. The high temperature and the low temperature branch were analysed separately. Both asymptotics display a negative temperature dependence in the intermediate temperature range, thereby illustrating that the 4-step mechanism contains the general features of the full kinetic mechanism.

Acknowledgement

This work was sponsored by the Commission of European Communities, by the National Swedish Board for Industrial and Technical Development (NUTEK) and by the Joint Research Council of European car manufacturers within the IDEA program.

REFERENCES

1. WESTBROOK, C. K., WARNATZ, J. AND PITZ, W. J.: Twenty-Second Symposium (International) on Combustion, p. 893, The Combustion Institute, 1989.
2. POLLARD, R. T.: Comprehensive Chemical Kinetics, (Bamford, C. H. and Tipper, C. F. H., Ed.), Vol 17, p. 249, American Elsevier, 1977.
3. CHEVALIER, C., LOUESSARD, P., MÜLLER, U. C. AND WARNATZ, J.: Int. Symp. on Diagnostics and Modeling of Combustion in Internal Engines, COMODIA 90, Kyoto The Japan Society of Mechanical Engineers, 1990.
4. COWART, J. S., KECK, J. C., HEYWOOD, J. B., WESTBROOK, C. K. AND PITZ, W. J.: Twenty-Third Symposium (International) on Combustion, p. 1055, The Combustion Institute, 1991.
5. WESTBROOK, C. K., PITZ, W. J. AND LEPPARD, W. R.: SAE paper No. 912314 (1991).
6. PITZ, W. J., WESTBROOK, C. K. AND LEPPARD, W. R.: SAE paper No. 912315 (1991).
7. COATS, C. M. AND WILLIAMS, A.: Seventeenth Symposium (International) on Combustion, p. 611, The Combustion Institute, 1979.
8. COX, R. A. AND COLE, J. A.: Combust. Flame 60, 109, 1985.

9. HALSTEAD, M. P., KIRSCH, L. J. AND QUINN, C. P.: *Combust. and Flame* 30, 45, 1977.
10. CIEZKI, H. AND ADOMEIT, G.: Shock tube investigation of self-ignition of fuel/air mixtures under engine conditions, to appear in *Combust. Flame*, 1992.
11. WARNATZ, J.: Private communication, 1991.
12. PETERS, N.: Systematic Reductions of Flame Kinetics; Principles and Details, in *Progress in Astronautics and Aeronautics* (KUHLE, A. L., BOWEN, J. R., LEYER, J. L. and BORISOV, A., Ed.), Vol 113, ISBN 0-930403-46-0, 1988.
13. MÜLLER, U. C. AND PETERS, N.: Development of reduced reaction schemes for ignition of Diesel fuels, IDEA-Programme, Internal Report, 1991.

COMMENTS

John Griffiths, University of Leeds, U.K. The numerical analysis of the 4-step scheme fails to capture the negative temperature dependence of ignition delay as shown by the computation of this full scheme and by the experimental results to which this work is matched. This qualitative flaw may be traced to the model itself. Ignition is brought about entirely by thermal feedback. There is no chain branching in any of the steps as written or reflected in the rate parameters (by encapsulating some complex dependence of fuel concentration, for example).

The negative temperature dependence of reaction rate in hydrocarbon oxidation originates in a kinetic interaction of the general structure,



as acknowledged in the introduction. However, this fundamental chain interaction cannot then be disregarded if reduced schemes are to capture correctly the features of hydrocarbon oxidation throughout the low and intermediate temperature range.

One rigorous test lies in computations of reaction rate performed under isothermal conditions. The model behaviour must show the classical "s," the shape of fuel consumption rate vs. ambient temperature. I do not believe the 4-step model would show such behaviour, but I urge the authors to try

this. Of course, thermal feedback is an additional (but definitely not exclusive) ingredient of the chain-thermal interaction that governs the complexity of two-stage ignition (and also oscillatory cool flames in other circumstances).

Author's Reply. We agree that in this ad-hoc-4-step model, chain branching is not retained. However, this is not the reason why the numerical calculations, differently from the asymptotic analysis, do not show the negative temperature dependence. We believe that it is the thermal interaction between the two parts of the mechanisms that smears out the negative temperature dependence. In the paper we mention a systematically reduced 16-step mechanism that uses the elementary kinetic rates. This mechanism retains the chain branching features and will be tested following your suggestions.

•

Dr. Christian Corre, ELF, France. I would like to know if this 4-step mechanism has already been tested in an industrial engine code (including fluid mechanics, heat transfer, . . .)?

Author's Reply. The model is being used in the framework of the IDEA collaboration within the SPEED program developed by Prof. Gosman.